Genes & Diseases (2019) 6, 68–77

Available online at www.sciencedirect.com

ScienceDirect

journal homepage: http://ees.elsevier.com/gendis/default.asp

FULL LENGTH ARTICLE

Neonatal overfeeding in mice aggravates the development of methionine and choline-deficient diet-induced steatohepatitis in adulthood

Juan Du [a,1], Xuemei Cao [a,1], Junlin Diao [a], Qijuan Zhang [b], Chuan Peng [a], Jibin Li [c], Xiaoqiu Xiao [a,*]

[a] *Laboratory of Lipid & Glucose Metabolism, PR China*
[b] *Department of Clinical Nutrition, The First Affiliated Hospital of Chongqing Medical University, PR China*
[c] *School of Public Health and Management, Chongqing Medical University, Research Center for Medicine and Social Development, Innovation Center for Social Risk Governance in Health, Chongqing, 400016, PR China*

Received 28 November 2017; accepted 23 December 2017
Available online 5 January 2018

KEYWORDS
Inflammation;
Insulin resistance;
Neonatal overfeeding;
Non-alcoholic steatohepatitis;
Obesity

Abstract Overfeeding in early life is associated with obesity and insulin resistance in adulthood. In the present study, a well-characterized mouse model was used to investigate whether neonatal overfeeding increases susceptibility to the development of non-alcoholic steatohepatitis (NASH) following feeding with a methionine and choline- deficient (MCD) diet. Neonatal overfeeding was induced by adjusting litters to 3 pups per dam (small litter size, SL) in contrast to 10 pups per dam as control (normal litter size, NL). At 11 weeks of age, mice were fed with standard (S) or a methionine and choline-deficient (MCD) diet for 4 weeks. Glucose tolerance tests, tissue staining with haematoxylin and eosin, oil-red O and immunohistochemistry for F4/80, reverse transcription-quantitative polymerase chain reaction (RT-qPCR) and western blotting were performed. Compared with NL mice, SL mice exhibited higher body weight gain from 2 weeks of age throughout adulthood, and more profound glucose intolerance as adults. Sterol regulatory element-binding protein 1c and fatty acid synthase mRNA expression levels in liver were upregulated in SL mice at 3 weeks of age. MCD diet induced typical NASH, especially in SL-MCD mice, evidenced by marked fat accumulation, macrovescular steatosis, ballooned hepatocytes, inflammatory cells infiltration and tumour necrosis factor-α mRNA upregulation in

* Corresponding author. Laboratory of Lipid & Glucose Metabolism, The First Affiliated Hospital of Chongqing Medical University, 1Youyi Road, Chongqing, 400016, PR China.
E-mail address: bshaw2001@163.com (X. Xiao).
Peer review under responsibility of Chongqing Medical University.
[1] These authors contribute equally to this study.

https://doi.org/10.1016/j.gendis.2017.12.008

the liver, as well as increased alanine aminotransferase and aspartate aminotransferase levels in the serum. There were no significant differences in liver fibrosis in all groups. Overfeeding during early life exhibited effect with administration of MCD diet in inducing adverse effects on the metabolic function and in promoting the progression of NASH in mice, possibly mediated through dysregulated lipid metabolism in hepatocytes and aggravated hepatic inflammation.

Introduction

Non-alcoholic fatty liver disease (NAFLD) is a sequent spectrum of disorders, including simple steatosis (fat accumulation), non-alcoholic steatohepatitis (NASH), cirrhosis and hepatocellular cancer, in the absence of alcohol abuse and other specific etiologies.[1–3] The prevalence of NAFLD is increasing at an alarming rate, especially in the obese populations. It is estimated that NAFLD affects one quarter of adults in the general populations and up to 70% of people with obesity or type 2 diabetes in developed countries.[4,5] Hepatic fat accumulation originates from three different sources: the delivery of dietary fat accounts for about 5% of liver fat, the delivery of extra-hepatic non-esterified fatty acids (NEFAs) to the liver contributes to 60% of liver fat, and the remainder of liver fat accumulation is influenced by hepatic de novo lipogenesis.[6] The early defect in the pathogenesis of NAFLD is thought to be insulin resistance.[1,7] Initial insulin resistance in adipose tissues facilitates the lipolysis and enhances fatty acid released from adipocytes. Increased fatty acid fluxes through the liver promote hepatic steatosis as well as hepatic gluconeogenesis, worsening hepatic and whole-body insulin resistance. In addition, adipose tissues produce a variety of inflammatory cytokines, such as tumour necrosis factor *(TNF)*-α and interleukin *(IL)-6*, which servea critical role in the propagation of NAFLD.[8,9] However, the specific etiopathogenesis of NAFLD remains poorly understood.

To gain insight into the pathogenesis of NAFLD and NASH, a variety of animal models have been developed that typically rely on genetic (such as the ob/ob or db/db mice) and dietary [such as the high fat and/or high fructose diets, and the methionine and choline-deficient diet (MCD) manipulations.[10,11] However, none of these models fully reflects the characteristic changes that develop in human NAFLD. Both ob/ob and db/db mice display the phenotypes of human metabolic syndrome in many aspects, but these mice do not spontaneously develop steatohepatitis or liver fibrosis.[12,13] In addition, mutations in the ob or its receptor genes are not prevalent in obese subjects or NASH patients, and leptin levels correlate poorly with the development of NASH.[14] High fat diet (HFD) has been widely used to induce hepatic steatosis and NASH. However, animals fed with HFD produce variable results with regard to the degree of steatosis, inflammation, and fibrosis. The inconsistencies in HFD-induced steatosis and NASH depend on animal species and strain, the dietary fat content, and the duration of treatment.[15,16] By contrast, MCD-induced hepatic steatosis and NASH is recognized as one of the best-studied animal models of NAFLD.[17–20] Rodents fed with MCD diets typically lose weight and gradually develop NASH, characterized by steatosis, prominent inflammation and hepatic lesions, mimicking the majority of manifestations observed in patients with NASH.[17–19]

It has been reported that neonatal overfeeding in animal models may be a predisposing factor for obesity, diabetes and other metabolic and respiratory-related diseases in later life.[21–25] These experimental findings are in accordance with the human observations that overfeeding during the early postnatal period may be considered as an essential risk factor for the onset of adult obesity and its complications. In addition, several studies have demonstrated that offspring from mothers fed with HFD during gestation and lactation are predisposed to develop a NASH-like phenotype, reinforcing that fetal programming is a critical risk factor for the development of NAFLD.[26–28] However, the relationship between neonatal overfeeding and NAFLD and its underlying mechanisms remain unclear. Therefore, we hypothesized that, as one of the risk factors, neonatal overfeeding may aggravate the development of NAFLD via altering the liver inflammation and lipid metabolism.

In the current study, neonatally overfed mice (nursed in small litters, SL) were fed with an MCD diet, and their hepatic phenotype was compared with postnatal normal fed (normal litters, NL) mice. The results demonstrated that SL mice developed more severe NASH compared with NL mice, featured by more prominent hepatic lipid accumulation and inflammation, accompanied with alterations in lipid metabolism-related genes and cytokines. These data indicated that neonatal overfeeding predisposed the mice to the development of insulin resistance and metabolic perturbations related to the onset and progression of NAFLD as adults. The current study may be beneficial to our understanding of the molecular mechanisms of NAFLD and highlight the importance of early intervention in the prevention of NAFLD.

Materials and methods

Animal model and experimental design

ICR strain mice were purchased from Jackson Laboratories (Ben Harbor, ME, USA) and maintained in a constant temperature room (23 $\pm$ 2 °C) with a 12-hr light/dark cycle. Pregnant ICR mice were maintained on standard chow, housed individually and monitored closely for the day of birth, which was considered as postnatal day 0 (P0). Their

male offspring were adjusted to 3 pups per litter (small litter size, SL) on P3 to build the model of neonatal overfeeding. Litters of 10 pups nurtured by one mother (normal litter size, NL) were regarded as control. Following weaning (at 3 weeks of age), all animals had free access to tap water and standard diets until 10 weeks of age. Glucose tolerance tests (GTT) were carried out between 10 and 11 weeks of age. Beginning at11 weeks of age, all animals were randomly divided into subgroups and fed with either standard diet (S) or methionine and choline-deficient diet (MCD; Dyets Inc., Bethlehem, PA, USA) for 4 weeks to form four groups of mice: NL-S, NL-MCD, SL-S and SL-MCD. Animals were sacrificed at 15 weeks of age (4 weeks after the start of the MCD diet). Samples of serum and the livers were obtained and stored at −80 °C. All animal care and experimental protocols were approved by the Ethical Principles in Animal Research adopted by the Chongqing Medical University for Animal Experimentation.

Glucose tolerance tests (GTTs)

GTTs were conducted as previous published.[29] Briefly, mice were fasted overnight and then were administered with glucose (2 g/kg body weight) through intraperitoneal injection. Blood glucose was measured from the tail vein using point-of-care blood glucose monitoring system (OneTouch SureStep Glucometer; Johnson &Johnson, New Brunswick, NJ, USA) at 0, 15, 30, 60 and 120 min following glucose administration.

Blood sampling and analysis

After the standard diet (S) or MCD diet for 4 weeks, blood was obtained by femoral artery cutting following anaesthesia and separated by centrifugation (1000 g, 4 °C, 15 min) to collect the serum. Serum samples were evaluated using an automatic biochemical analyser (ADVIA 2400 chemistry system; Siemens AG, Munich, Germany). Serum insulin levels were measured using a mouse insulin ELISA kit from Abbexa Ltd (Cambridge, UK, Cat no: abx154219).

Observation of hepatic ultrastructure

Hepatic samples for transmission electron microscopy analysis were collected from 3-week-old NL and SL mice based on our standard protocol. The liver tissues were isolated, immersed in 4% electron microscopy-purpose glutaraldehyde for 2 h, and stored at 4 °C. The samples were then processed for gradient dehydration, Resin 812 covering, and slicing into ultrathin layers with 60 nm thickness. Ultrathin sections were stained with uranyl acetate and lead citrate overnight and observed using aHitachi-7500 transmission electron microscope (Hitachi, Ltd., Tokyo, Japan).

Histological analysis

Livers from 15-week-old mouse were fixed in 4% paraformaldehyde, and then embedded in paraffin. Haematoxylin and eosin (HE) staining was performed on paraffin sections (6 μM in thickness) for 48 h. Sirius Red staining and immunohistochemistry analysis for F4/80 (cat no. ab6640; Abcam, Cambridge, UK) and α-smooth muscle actin (α-SMA; cat no. ab5694; Abcam) were performed based on our standard procedures. The paraffin sections were washed slides 3 times for 5 min in xylene to deparaffinizate and dehydrate using graded ethanol. After routinely antigen retrieval which including heat-mediated retrieval in citrate buffer, add 100 μl per slide of blocking solution for 30 min at room temperature and then after draining it from slides apply 100 μl per slide of diluted primary antibody (Dilution ratio-1:50) overnight at 4 °C. Apply conjugated polyclonal IgG-HRP antibody in Rat two step assay kit (PV6000, ZSGB-BIO, China) for 30 min at room temperature. Apply DAB Color Kit (PV6000-D, ZSGB-BIO, China) by following manufacturer's instructions and be observed by Biological microscope DM4000B (Lecia, Germany). Oil-red O staining was performed on frozen sections. They were washed with PBS and stained with freshly diluted Oil Red O working solution (0.5% Oil Red O in isopropanol: H_2O = 3:2) for 1 h, and counterstained with haematoxylin for 3 min. An experienced pathologist blinded to the treatment groups evaluated the liver histology. Histological scoring was based on the Brunt classification,[30] and steatosis was graded as follows: 0, 0—5% of hepatocytes affected; 1, 5—30% of hepatocytes affected; 2, 30—60% of hepatocytes affected; and 3,>60% of hepatocytes affected. Inflammatory grade was scored on a scale of 0—4 as follows: *0, no inflammation; 1, sparse zone three inflammation; 2, mild focal zone three hepatocyte inflammation; 3, moderate zone three hepatocyte inflammation; and 4, severe zone three hepatocyte inflammation*. Balloon degeneration was scored on an arbitrary scale of 0—4 as follows: *0, none; 1, minimal (<10%); 2, mild (10—33%); 3, moderate (33—66%); and 4, severe (>66%)*. All histological scores were performed by six random fields per sample under low-power fields (magnification, ×10) (n = 4 samples per group).

RNA extraction and reverse transcription-quantitative polymerase chain reaction (RT-qPCR)

Total RNA was extracted from snap frozen liver tissues including 3-week-old and 15-week-old with TRIzol reagent (Takara Biotechnology Co., Ltd., Dalian, China). The PrimeScript RT reagent kit (Takara Biotechnology Co., Ltd.) was used for cDNA synthesis. qPCR analysis was performed using the SYBR Green Premix Ex Taq II kit (Takara Biotechnology Co., Ltd.) on aCFX96 real-time PCR detection system (Bio-Rad Laboratories, Inc., Hercules, CA, USA). qPCR reactions were performed in triplicate in a 25 μl final reaction volume that included 12.5 μl SYBR Green premix solution, 0.25 μl of forward primer, 0.25 μl of reverse primer, 2 μl of cDNA, and 10 μl ddH_2O. Thermocycling conditions were as follows:*1. 95.0 °C for 0:30; 2. 95.0 °C for 0:05; 3. 60 °C for 0:34 + Plate Read ; 4. Go to 2, 39 more times; 5. Melt Curve 65.0 to 95.0 °C ,increment 0.5 °C, for 0.05 + Plate Read. End.* The sequences of the primers used in the present study are listed in Table 1. The comparative cycle time (Cq) method (the $2^{-\Delta\Delta Ct}$ method) was used to determine fold differences between samples.[31] The comparative Cq method determines the amount of the target gene normalized to an endogenous reference (*GAPDH*) and relative to a calibrator.

Table 1 Sequences of primers used for reverse transcription-quantitative polymerase chain reaction.

Gene	Accession number	Primer	Sequence (5'-3')
Srebp1c	NM_011480.3	Forward	TGGCTTGGTGATGCTATGTTG
		Reverse	GACCATCAAGGCCCCTCA A
Fasn	NM_007988.3	Forward	CCCAAGAACCAACAAGATGAA
		Reverse	AATCAAGGCAAGACATAGCGA
Acc-1	NM_133360.2	Forward	GGCAGCTCTGGAGGTGTATG
		Reverse	TCCTTAAGCTGGCGGTGTT
TNF-α	NM_013693.2	Forward	CTGAGGTCAATCTGCCCAAGTAC
		Reverse	CTTCACAGAGCAATGACTCCAAAG
IL-6	NM_031168.1	Forward	CTGCAAGAGACTTCCATCCAGTT
		Reverse	AGGTAGGGAAGGCCGTGGTT
GAPDH	NM_001244854.1	Forward	CAAGGCATCCATGACAACTTTG
		Reverse	GGCCATCCACAGTCTTCTGG

Srebp1c, sterol regulatory element-binding protein 1c; *Fasn*, fatty acid synthase; *Acc-1*, Acetyl-CoA carboxylase-1; *TNF-α*, tumour necrosis factor-α; *IL-6*, interleukin-6.

Protein extraction and western blotting

Frozen liver tissues from 3-week-old mouse were sliced and thawed in ice-cold lysis buffer (20 mM Tris-Cl pH7.5, 150 mM NaCl, 1% Triton-X, 10 mM NaF, and 1 mM EDTA) supplemented with 1 mM Na_3VO_4, 1 mM PMSF, and protease inhibitor cocktail (Santa Cruz Biotechnology, Inc., Dallas, TX, USA). Protein concentrations were determined using the bicinchoninic acid protein assay. Aliquots of 40ug Protein were separated electrophoretic ally by 8% SDS-PAGE, and blotted onto polyvinyl Dene fluoride membranes (Bio-Rad Laboratories, Inc.). The blots were incubated overnight at 4 °C with primary mouse anti-SREBP1 antibody (1:1000; Abcam; ab28481) or primary rabbit anti-actin antibody (1:2000;CST;#4967) and horseradish peroxidase-conjugated anti-mouse secondary antibody (1:4000;Abcam; ab131368) or anti-rabbit secondary antibody (1:4000;CST;#7074). Signals on the membranes were visualized with an enhanced chemiluminescence western blot detection kit (EMD Millipore; Billerica, MA, USA). Signal intensities were quantified using the Quantity One analysis software, version 4.6.9 (Bio-Rad Laboratories, Inc.).

Statistical analysis

Data were analysed with the Graphpad Prism version 5.0 software (GraphPad Software, Inc., La Jolla, CA, USA). All results were expressed as mean ± standard error of the mean. Differences between two groups were compared by paired sample t-test. Differences between the NL and SL groups under different diets (S and MCD) were compared two-way analysis of variance. $P < 0.05$ was considered to indicate a statistically significant difference.

Results

Neonatal overfeeding induces immediate weight gain and hepatic lipogenesis

To assess the influence of neonatal overfeeding on body weight and lipogenesis in the liver of infant mice prior to weaning, the body weight of NL and SL mice was measured from the day of birth up to 3 weeks of age. SL pups were significantly heavier than NL pups beginning at 2 weeks of age (Fig. 1A) and exhibited significant hyperinsulinemia (Fig. 1B). Hepatic mRNA expression levels of sterol regulatory element-binding protein 1c (*Srebp1c*) and fatty acid synthase (*Fasn*) in SL pups were significantly upregulated compared with NL pups (Fig. 1C), accompanied with increased maturated Srebp1c protein levels (Fig. 1C). *Acc-1* was mildly increased compared with NL pups (Fig. 1C). These genes played an important regulatory role in the synthesis of fatty acids. To sum up, these results showed the synthesis of fatty acids of SL pups was more significant than NL pups. Ultrastructural analysis with transmission electron microscopy revealed that the livers of infant SL mice werecharacterized by an apparent decrease in intracytoplasmic organelles, fat deposition and liver vacuolization (Fig. 1D). In addition, rough endoplasmic reticulum and nuclei, and swollen mitochondria were observed in hepatocytes from SL mice (Fig. 1D). These results suggested that neonatal overfeeding may accelerate body weight gain, hyperinsulinemia and de novo lipogenesis, resulting in hepatic lipid deposition in infancy.

Neonatal overfeeding induces persistent weight gain and glucose intolerance

Following weaning, SL mice were heavier than NL mice until young adulthood (Fig. 2A). Fasting glucose levels did not differ between SL and NL mice at 10 weeks of age (Fig. 1B). However, blood glucose concentrations in SL mice were significantly higher compared with NL mice at 30 and 60 min following glucose loading (Fig. 2B). These data suggested that neonatal overfeeding had adverse impacts on glucose homeostasis in later stages.

MCD diet feeding leads to weight loss and changes in serum lipid profiles

SL and NL mice at 11 weeks of age were randomly divided into two subgroups and fed with either S or MCD diets for a

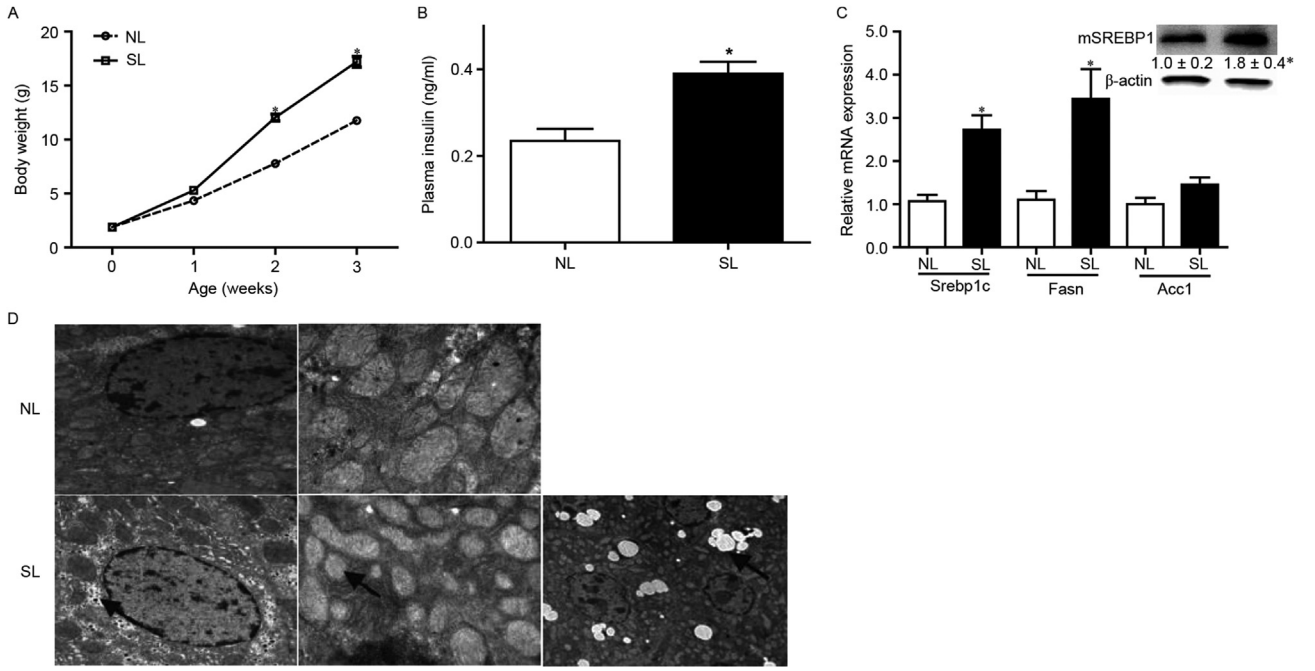

Figure 1 Neonatal overfeeding induces immediate weight gain and hepatic lipogenesis. (A) Body weight was measured once a week from birth to 3 weeks of age ($n = 50$). (B) Serum insulin levels were measured using a mouse insulin ELISA. (C) mRNA expression levels of Srebp1c, Fasn and Acc-1 were detected by reverse transcription-quantitative polymerase chain reaction (n = 6—8). Protein expression levels of mSREBP1 were determined by western blotting ($n = 4$). (D) Representative images of hepatocyte ultrastructure from NL and SL mice. Ultrastructural analysis with transmission electron microscopy revealed that the liver of infant SL mice exhibited an apparent increase in intracytoplasmic fat deposition (arrow on right lower panel), swollen mitochondria (arrow on middle lower panel) and glycogen deposition (arrow on left lower panel). Data were presented as mean ± standard error of the mean. $*p < 0.05$ vs NL. Srebp1c, sterol regulatory element-binding protein 1c; *Fasn*, fatty acid synthase; *Acc-1*, Acetyl-CoA carboxylase-1; m, maturated; NL, normal litter size; SL, small litter size.

total of 4 weeks. Following feeding with the MCD diet, both SL and NL mice exhibited reduced body weight compared with controls (Fig. 2C), which is consistent with previous studies.[32,33] Although liver weight did not change (Fig. 2D), the ratio of liver weight to body weight was increased in NL-MCD and SL-MCD mice compared with the respective groups fed normal diets (Fig. 2E). Serum glucose, triglyceride, total cholesterol, low-density lipoprotein and high-density lipoprotein levels were significantly decreased in mice fed MCD diets compared with mice fed normal diets (Fig. 3). These alterations were regarded as typical characteristics of MCD-induced NASH, validating the induction of NASH in the present study.

Neonatal overfeeding aggravates hepatic lipid accumulation and injury following MCD diet feeding

Typical NASH is characterized by macrovascular steatosis, ballooning, inflammation, macrophage recruitment, and fibrosis (28). HE (Fig. 4A, upper panels) and oil-red O (Fig. 4A, lower panels) staining was performed in liver tissue sections from the four experimental mouse groups. The results demonstrated that NL-S livers exhibited a normal morphology and no visible steatosis, while SL-S livers exhibited mild steatosis and cellular swelling without obvious signs of ballooning and inflammatory cell recruitment. MCD diet feeding resulted in typical NASH, evidenced by hepatic fat accumulation, increased ballooning and inflammatory cell recruitment, in both NL and SL livers. However, more severe signs were observed in the SL mice fed with MCD diets. Compared with NL-MCD mice, SL-MCD mice displayed a higher steatosis score (Fig. 4B), indicating that the NASH severity was higher in SL-MCD mice. Consistently, serum alanine aminotransferase (ALT) and aspartate aminotransferase (AST)activities were significantly increased in both NL-MCD and SL-MCD mice compared with the respective mice fed with a normal diet, with the highest activities evident in the SL-MCD mice (Fig. 4C and D). These data suggested that neonatal overfeeding aggravated the fat accumulation and deteriorated the liver pathology in mice. Therefore, the present results demonstrated an additive effect between neonatal overfeeding and MCD diet in regards to steatosis scores and liver injury.

Neonatal overfeeding promotes hepatic inflammation following MCD dietfeeding

F4/80 staining of liver tissue sections from the four experimental mouse groups revealed that the NL-S and SL-S livers had no obvious macrophages (Fig. 5A). Feeding with a MCD diet resulted in an obvious macrophage recruitment, especially in the SL-MCD livers (Fig. 5A and B). Macrophages localized predominantly around hepatocytes in the NL-MCD livers (Fig. 5A). However, in SL-MCD, macrophages gathered

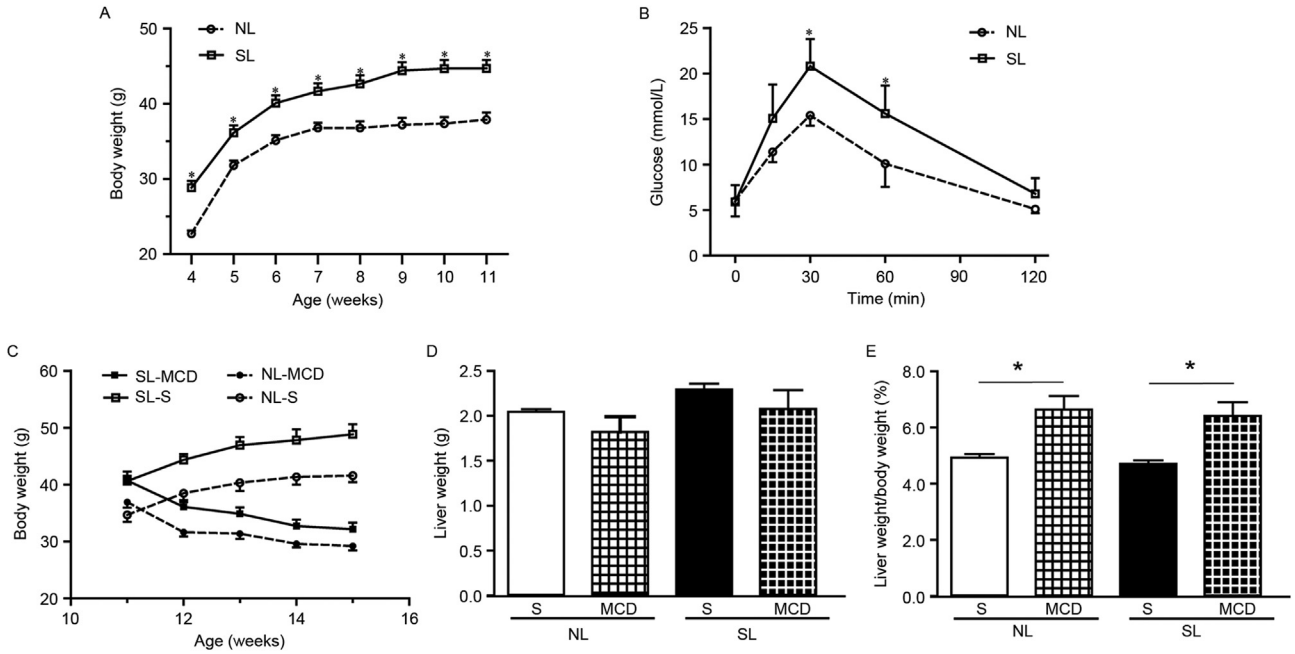

Figure 2 Neonatal overfeeding induces persistent weight gain and glucose intolerance, while the MCD diet reduces body weight. (A) Body weight of NL and SL mice we measured weekly from weaning to 11 weeks of age ($n = 30$). (B) Glucose tolerance tests at 10 weeks of age (n = 5—6). (C) Body weight of mice starting at 11 weeks of age and fed with MCD or S diet for 4 weeks. (D) Liver weight of mice fed with MCD diet. (E) Liver weight/body weight ratio of mice fed with MCD diet. CE, data were presented as mean ± standard error of the mean (n = 6—8). $*p < 0.05$ vs. SL or indicated by lines. MCD, methionine and choline-deficient diet; NL, normal litter size; SL, small litter size; S, standard diet.

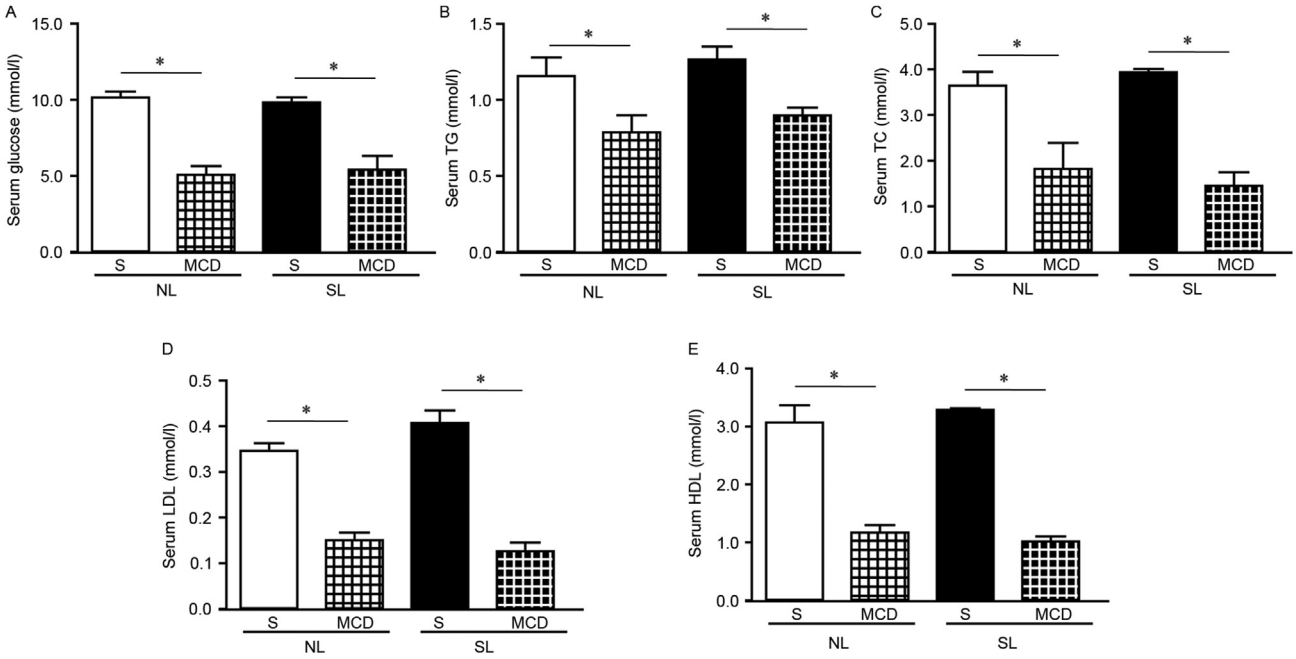

Figure 3 MCD diet feeding alters the serum biochemical index in both NL and SL mice. Serum levels for (A) glucose, (B) TG, (C) TC, (D) LDL, (E) HDL were measured in the experimental groups. Data were presented as mean ± standard error of the mean (n = 5—6). $*p < 0.05$ with comparisons indicated by lines. MCD, methionine and choline-deficient diet; NL, normal litter size; SL, small litter size; TG, triglyceride; TC, total cholesterol; LDL, low-density lipoprotein; HDL, high-density lipoprotein; S, standard diet.

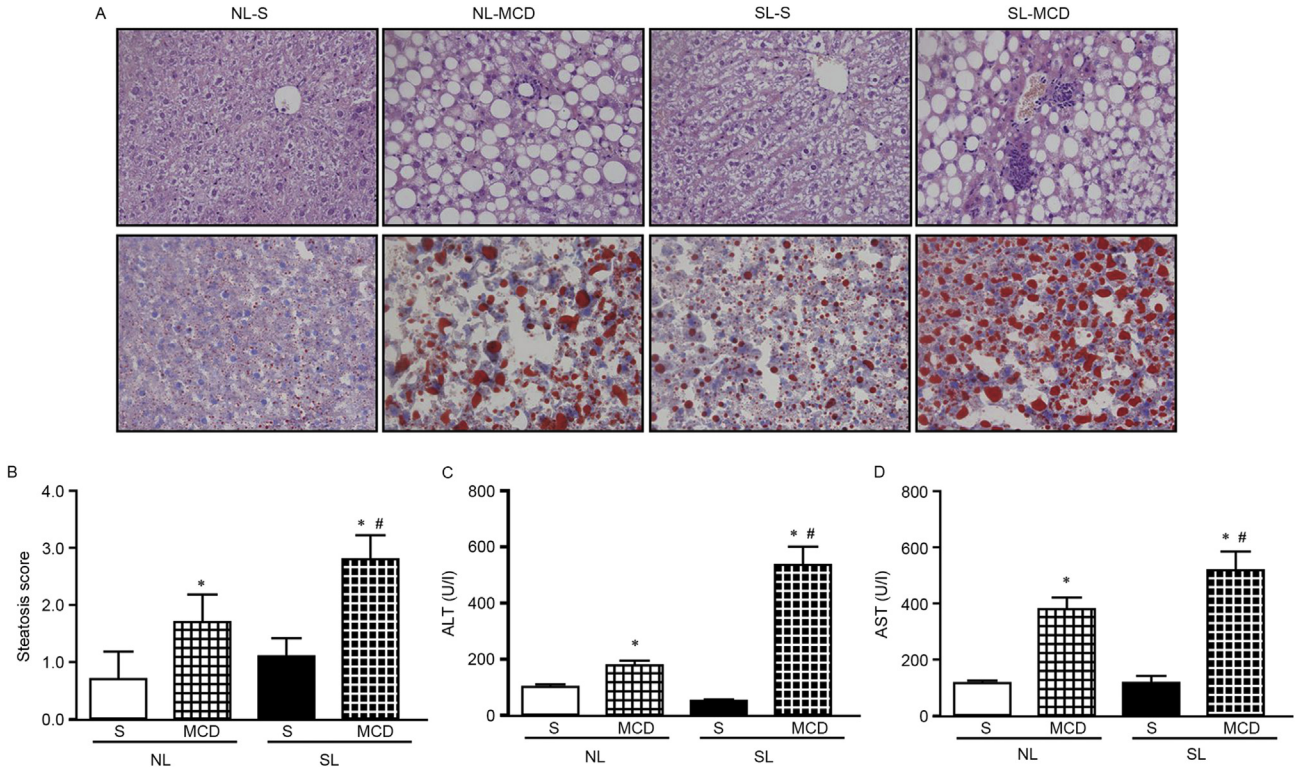

Figure 4 Neonatal overfeeding aggravates hepatic lipid accumulation and impairment following feeding with MCD diet. (A) Haematoxylin and eosin (upper panels) and oil-red O (lower panels) staining examining lipid accumulation and inflammation. (B) Quantification score of hepatic steatosis. (C) Serum ALT levels. (D) Serum AST levels. Data were presented as mean ± standard error of the mean (n = 5–6). $*p < 0.05$ vs. S; $^{\#}p < 0.05$ vs NL-MCD. MCD, methionine and choline-deficient diet; ALT, alanine aminotransferase; AST, aspartate aminotransferase; NL, normal litter size; SL, small litter size; S, standard diet.

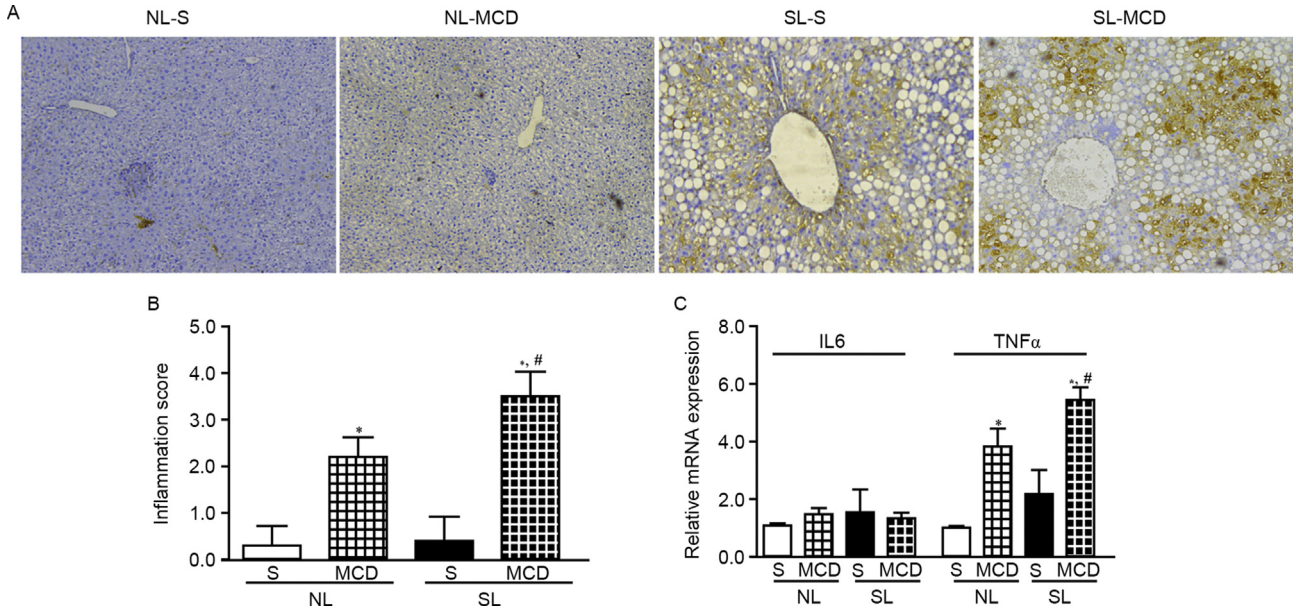

Figure 5 Neonatal overfeeding promotes hepatic inflammation following feeding with MCD diet. (A) Macrophages in the liver were detected by F4/80 immunohistochemical staining. (B) Quantified inflammation score. (C) Expression of IL-6 and TNF-α was determined by reverse transcription-quantitative polymerase chain reaction. Data were presented as mean ± standard error of the mean (n = 5–6). $*p < 0.05$ vs. S; $^{\#}p < 0.05$ vs NL-MCD. MCD, methionine and choline-deficient diet; IL, interleukin; TNF, tumour necrosis factor; NL, normal litter size; SL, small litter size; S, standard diet.

around hepatocytes more seriously (Fig. 5A). To assess whether proinflammatory cytokines were involved in the MCD-mediated increased hepatic macrophage recruitment, the mRNA expression levels of IL-6 and TNF-α were assessed. *TNF-α*, but not *IL-6*, exhibited a significant increase in mRNA expression in the MCF-fed mice, that was consistent with the inflammation score (Fig. 5C). These data suggested an additive effect between neonatal overfeeding and MCD diet leading to hepatic inflammation.

Discussion

Previous reports from both epidemiological human and experimental animal studies have demonstrated that overfeeding during fetal and neonatal life may lead to a variety of metabolic-related disorders in adulthood, and neonatal overfeeding represents a predisposing factor for obesity, diabetes susceptibility and other metabolic and respiratory diseases in later life.[22–26] Rodent animal models of neonatal overfeeding via reduced litter size have been widely used in studies of hypothalamic feeding circuitry, hypertension, renal and respiratory functions. Neonatally overfed mice were characterized by persistent increased weight and early onset of obesity, hyperleptinemia, hyperinsulinemia, glucose intolerance, impaired hypothalamic feeding circuitry, impaired norepinephrine turnover and brown adipose tissue thermogenesis.[21–23,25] Under obese state, inadequate adipose tissue expandability leads to an increased presence of hypertrophic adipocytes, which further activates the endoplasmic reticulum stress and inflammatory pathways and induces insulin resistance in adipocytes. These effects induce an increase in circulating free fatty acids and a decrease in lipid utilization by insulin-sensitive organs, subsequently leading to hepatic lipid accumulation and hepatic injury.[34] However, there is little direct evidence in support of the relationship between overfeeding at early life stage and adult NAFLD. Thereby, the present study explored the relationship between early postnatal overfeeding and the development and progression of NAFLD.

Previous studies from our group and others have demonstrated that neonatal overfeeding during the period of lactation induced rapid weight gain beginning at2 weeks of age and the higher body weight persisted into adulthood.[22,23,25] The present study aimed to examine the hepatic consequences of neonatal overfeeding under conditions of standard or MCD diets. Sterol regulatory element-binding proteins (SREBPs) are a family of membrane-bound transcription factors that regulate cholesterol and fatty acid homeostasis. There are three Srebp isoforms designated *Srebp1a*, *Srebp1c*, and *Srebp-2*. *Srebp1c*, mainly expressed in the liver, is a major transcriptional factor of lipid synthesis-related genes, such as *Fasn* and stearoyl-CoA desaturase-1.[35] In the present study, *Srebp1c* and *Fasn* were demonstrated to be upregulated in SL mice compared with NL mice, as early as at 3 weeks of age, indicating an active process of fatty acid de novo synthesis in SL infant mice. In addition, ultrastructural observation with transmission electron microscopy demonstrated that the liver from infant SL mice displayed nuclear deformation and mitochondrial swelling with obvious intracytoplasmic glycogen and lipid deposition. Following weaning, SL mice demonstrated a persistent higher body weight even though they were maintained under the identical diets with their counterparts, and gradually developed glucose intolerance. These findings were generally in agreement with previous reports.[36,37] Furthermore, even fed with standard diets, the SL mice developed obvious simple steatosis compared with NL mice in adulthood. To explore whether neonatal overfeeding increased susceptibility to subsequent metabolic stress, the SL and NL mice were challenged with MCD diets. Mice fed MCD diets develop measurable hepatic steatosis by 2—4 weeks which progresses to inflammation, hepatic lesion and fibrosis shortly thereafter, typically displaying pathological and biochemical similarities with human steatohepatitis, although it does not induce insulin resistance.[38,39] The mice feeding with the MCD diet, both SL and NL mice exhibited reduced body weight compared with controls, and neonatal overfeeding through SL exacerbated MCD diet induced hepatic inflammation and injury. If using a high-fat diet, you will gain weight gain rather than weight loss. We have studied that high-fat diet induced some of the metabolic changes in the Ref. [23], and MCD specificity induced NASH. STZ-induced Type 1 diabetes was not related to NASH.These alterations were regarded as typical characteristics of MCD-induced NASH, validating the induction of NASH in the present study. In the present study, following 4 weeks of MCD diet feeding, SL mice displayed marked liver injury (evidenced by higher serum levels of ALT and AST) and more severe hepatic ballooning and inflammatory response (evidenced by macrophage recruitment and upregulated TNF-α), compared with NL mice. Of note, signs of NASH were further exaggerated in mice that were exposed to neonatal overfeeding. This is, to our knowledge, the first report to demonstrate the direct evidence between early overfeeding and increased susceptibility of NAFLD.

Inflammation is one of the important features in the development of NASH. Recent studies have reported that liver resident macrophages, such as Kupffer cells, servea pivotal role in triggering liver inflammation and hepatic damage, and the increase of TNF-α-producing Kupffer cells in the liver is crucial for the early phase of NASH development.[40,41] Neonatally overfed mice had already displayed obvious adiposity and insulin resistance prior to the MCD diet feeding. On this insulin-resistant background, the subsequent MCD dietary models of NASH may clarify the causal relationship of insulin resistance in the development of NASH. In the present study, more severe macrophage infiltration and upregulation of *TNF-α* mRNA expression were observed in the liver of SL mice following feeding with MCD diets. The present results were in accordance with several previous findings. For instance, a time course study with high fat diets (HFD) demonstrated that increased macrophage and upregulated cytokine transcripts occurred in adipose tissues prior to their appearance in the liver.[42] In addition, the MCD diet-induced steatohepatitis was accelerated in obese OLETF rats compared with lean LETO rats, and the combination of MCD with HFD diets further enhanced insulin resistance and led to rapid development of pre-cirrhosis in OLETF rats. By contrast, pioglitazone attenuated the MCD diet-induced steatohepatitis in OLETF

rats, but not in LETO rats, by reversing the underlying pathogenesis involved in this model through improvement of insulin resistance.[43] Furthermore, obese (ob/ob) and diabetic (db/db) mice, which are leptin and leptin receptor deficient respectively, develop marked hepatic inflammation and steatohepatitis following MCD diet feeding.[12,13,44] All these results indicated that insulin resistance and prediabetes may be the critical determinants of susceptibility and severity in accelerated inflammation and another pathologic spectrum of NASH.

Fibrosis is an important hallmark of NASH due to the activation of hepatic stellate cells and excessive deposition of extracellular matrix proteins.[45,46] Notably, no obvious liver fibrosis was observed in the present study, based on either Sirius Red staining, α-SMA immunohistochemistry, or TGF-β1 gene expression (data not shown). One possible explanation for this discrepancy may be the differences in the period of MCD diet feeding and the animal strains.[10,47] Previous studies have reported that at least 5 weeks of MCD diet feeding is required to induce distinct liver fibrosis (30,36). In addition, the magnitude of liver injury and the extent of histological changes in the liver varied greatly among the different animal species (10, 46). Further studies will be required to clarify these experimental differences by extending the period of MCD diet feeding and comparing between ICR mice and inbred strains of mice, such as the C57BL/6J.

In summary, obesity induced by early life overfeeding enhances hepatic fat accumulation, inflammation and liver injury and promotes the progression of NAFLD. The present study demonstrated an additive effect between neonatal overfeeding and metabolic insults (MCD diet feeding) in induction of hepatic steatosis and inflammation. Future studies including a pair-feeding experimental design, by pairing the daily food intake of SL mice with this of NL mice at the same age, and examining DNA methylation patterns, are underway in our group. These studies may increase our understanding of the molecular mechanism underlying NAFLD and highlight the importance of early intervention in the prevention of NAFLD.

Conflict of interest

The authors declare no conflict of interest.

Acknowledgements

The present work was supported by the National Natural Science Foundation of China (grant nos. 81270947 and 81570763, to XX), the National Program on Key Basic Research Project of China (973 Program; grant no. 2012CB517505, to XX), and the Fundamental Science and Advanced Technology Research of Chongqing (Major Project, grant no. CSTC2015jcyjB0146).

References

1. Day CP, James OF. Steatohepatitis: a tale of two "hits"? *Gastroenterology*. 1998;114(4):842—845.
2. Byrne CD. Ectopic fat, insulin resistance and non-alcoholic fatty liver disease. *Proc Nutr Soc*. 2013;72(4):412—419.
3. Calzadilla Bertot L, Adams LA. The natural course of non-alcoholic fatty liver disease. *Int J Mol Sci*. 2016;17(5).
4. Milic S, Lulic D, Stimac D. Non-alcoholic fatty liver disease and obesity: biochemical, metabolic and clinical presentations. *World J Gastroenterol*. 2014;20(28):9330—9337.
5. Sherif ZA, Saeed A, Ghavimi S, et al. Global epidemiology of nonalcoholic fatty liver disease and perspectives on US minority populations. *Dig Dis Sci*. 2016;61(5, Sp. Iss. SI):1214—1225.
6. Byrne CD, Olufadi R, Bruce KD, Cagampang FR, Ahmed MH. Metabolic disturbances in non-alcoholic fatty liver disease. *Clin Sci (Lond)*. 2009;116(7):539—564.
7. Asrih M, Jornayvaz FR. Metabolic syndrome and nonalcoholic fatty liver disease: is insulin resistance the link? Molecular and cellular endocrinology. 2015;418(Pt 1):55—65.
8. Fujii H, Kawada N. Inflammation and fibrogenesis in steatohepatitis. *J Gastroenterol*. 2012;47(3):215—225.
9. Duarte N, Coelho IC, Patarrao RS, Almeida JI, Penha-Goncalves C, Macedo MP. How inflammation impinges on NAFLD: a role for Kupffer cells. *Int Biomed Res*. 2015;2015:984578.
10. Kirsch R, Clarkson V, Shephard EG, et al. Rodent nutritional model of non-alcoholic steatohepatitis: species, strain and sex difference studies. *J Gastroenterol Hepatol*. 2003;18(11):1272—1282.
11. Takahashi Y, Soejima Y, Fukusato T. Animal models of nonalcoholic fatty liver disease/nonalcoholic steatohepatitis. *World J Gastroenterol WJG*. 2012;18(19):2300—2308.
12. Leclercq IA, Farrell GC, Schriemer R, Robertson GR. Leptin is essential for the hepatic fibrogenic response to chronic liver injury. *J Hepatol*. 2002;37(2):206—213.
13. Sahai A, Malladi P, Pan X, et al. Obese and diabetic db/db mice develop marked liver fibrosis in a model of nonalcoholic steatohepatitis: role of short-form leptin receptors and osteopontin. *Am J Physiol Gastrointest Liver Physiol*. 2004;287(5):G1035—G1043.
14. Chalasani N, Crabb DW, Cummings OW, et al. Does leptin play a role in the pathogenesis of human nonalcoholic steatohepatitis? *Am J Gastroenterol*. 2003;98(12):2771—2776.
15. Larter CZ, Yeh MM. Animal models of NASH: getting both pathology and metabolic context right. *J Gastroenterol Hepatol*. 2008;23(11):1635—1648.
16. Nishikawa S, Yasoshima A, Doi K, Nakayama H, Uetsuka K. Involvement of sex, strain and age factors in high fat diet-induced obesity in C57BL6J and BALB/cA mice. *Exp Anim (Tokyo)*. 2007;56(4):263—272.
17. Macfarlane DP, Zou X, Andrew R, et al. Metabolic pathways promoting intrahepatic fatty acid accumulation in methionine and choline deficiency: implications for the pathogenesis of steatohepatitis. *Am J Physiol Endocrinol Metabol*. 2011;300(2):E402—E409.
18. Park H-S, Jeon BH, Woo SH, et al. Time-dependent changes in lipid metabolism in mice with methionine choline deficiency-induced fatty liver disease. *Mol Cell*. 2011;32(6):571—577.
19. Soon Jr RK, Yan JS, Grenert JP, Maher JJ. Stress signaling in the methionine-choline-deficient model of murine fatty liver disease. *Gastroenterology*. 2010;139(5):1730.
20. Varela-Rey M, Embade N, Ariz U, Lu SC, Mato JM, Martinez-Chantar ML. Non-alcoholic steatohepatitis and animal models: understanding the human disease. *Int J Biochem Cell Biol*. 2009;41(5):969—976.
21. Xiao XQ, Williams SM, Grayson BE, et al. Excess weight gain during the early postnatal period is associated with permanent reprogramming of brown adipose tissue adaptive thermogenesis. *Endocrinology*. 2007;148(9):4150—4159.
22. Habbout A, Delemasure S, Goirand F, et al. Postnatal overfeeding in rats leads to moderate overweight and to cardiometabolic and oxidative alterations in adulthood. *Biochimie*. 2012;94(1):117—124.

23. Liu Z, Lim CY, Su MY-F, et al. Neonatal overnutrition in mice exacerbates high-fat diet-induced metabolic perturbations. *J Endocrinol*. 2013;219(2):131—143.
24. Ye Z, Huang Y, Liu D, et al. Obesity induced by neonatal overfeeding worsens airway hyperresponsiveness and inflammation. *PLoS One*. 2012;7(10), e47013.
25. Glavas MM, Kirigiti MA, Xiao XQ, et al. Early overnutrition results in early-onset arcuate leptin resistance and increased sensitivity to high-fat diet. *Endocrinology*. 2010;151(4):1598—1610.
26. Bruce KD, Cagampang FR, Argenton M, et al. Maternal high-fat feeding primes steatohepatitis in adult mice offspring, involving mitochondrial dysfunction and altered lipogenesis gene expression. *Hepatology*. 2009;50(6):1796—1808.
27. Ashino NG, Saito KN, Souza FD, et al. Maternal high-fat feeding through pregnancy and lactation predisposes mouse offspring to molecular insulin resistance and fatty liver. *J Nutr Biochem*. 2012;23(4):341—348.
28. Mouralidarane A, Soeda J, Visconti-Pugmire C, et al. Maternal obesity programs offspring nonalcoholic fatty liver disease by innate immune dysfunction in mice. *Hepatol (Baltimore Md)*. 2013;58(1):128—138.
29. Song Y, Li J, Zhao Y, et al. Severe maternal hyperglycemia exacerbates the development of insulin resistance and fatty liver in the offspring on high fat diet. *Exp Diabetes Res*. 2012;2012:254976.
30. Brunt EM, Janney CG, Di Bisceglie AM, Neuschwander-Tetri BA, Bacon BR. Nonalcoholic steatohepatitis: a proposal for grading and staging the histological lesions. *Am J Gastroenterol*. 1999;94(9):2467—2474.
31. Livak Kenneth J, Schmittgen Thomas D. Analysis of relative gene expression data using real- time quantitative PCR and the 2 CT method. *Methods*. 2001;25:402—408.
32. Caballero F, Fernandez A, Matias N, et al. Specific contribution of methionine and choline in nutritional nonalcoholic steatohepatitis: impact on mitochondrial S-adenosyl-L-methionine and glutathione. *J Biol Chem*. 2010;285(24):18528—18536.
33. Rezazadeh A, Yazdanparast R, Molaei M. Amelioration of diet-induced nonalcoholic steatohepatitis in rats by Mn-salen complexes via reduction of oxidative stress. *J Biomed Sci*. 2012;19(1):26.
34. Mollica MP, Lionetti L, Putti R, Cavaliere G, Gaita M, Barletta A. From chronic overfeeding to hepatic injury: role of endoplasmic reticulum stress and inflammation. *Nutr Metabol Cardiovasc Dis*. 2011;21(3):222—230.
35. Eberle D, Hegarty B, Bossard P, Ferre P, Foufelle F. SREBP transcription factors: master regulators of lipid homeostasis. *Biochimie (Paris)*. 2004;86(11):839—848.
36. Plagemann A, Heidrich I, Gotz F, Rohde W, Dorner G. Obesity and enhanced diabetes and cardiovascular risk in adult rats due to early postnatal overfeeding. *Exp Clin Endocrinol*. 1992;99(3):154—158.
37. Wang H, Ji J, Yu Y, et al. Neonatal overfeeding in female mice predisposes the development of obesity in their male offspring via altered central leptin signalling. *J Neuroendocrinol*. 2015;27(7):600—608.
38. Larter CZ, Yeh MM, Williams J, Bell-Anderson KS, Farrell GC. MCD-induced steatohepatitis is associated with hepatic adiponectin resistance and adipogenic transformation of hepatocytes. *J Hepatol*. 2008;49(3):407—416.
39. Pelz S, Stock P, Bruckner S, Christ B. A methionine-choline-deficient diet elicits NASH in the immunodeficient mouse featuring a model for hepatic cell transplantation. *Exp Cell Res*. 2012;318(3):276—287.
40. Tosello-Trampont AC, Landes SG, Nguyen V, Novobrantseva TI, Hahn YS. Kuppfer cells trigger nonalcoholic steatohepatitis development in diet-induced mouse model through tumor necrosis factor-alpha production. *J Biol Chem*. 2012;287(48):40161—40172.
41. Lanthier N. Targeting Kupffer cells in non-alcoholic fatty liver disease/non-alcoholic steatohepatitis: why and how? *World J Hepatol*. 2015;7(19):2184—2188.
42. Stanton MC, Chen S-C, Jackson JV, et al. Inflammatory Signals shift from adipose to liver during high fat feeding and influence the development of steatohepatitis in mice. *J Inflamm London*. 2011;8(8). Article No.: 8.
43. Ota T, Takamura T, Kurita S, et al. Insulin resistance accelerates a dietary rat model of nonalcoholic steatohepatitis. *Gastroenterology*. 2007;132(1):282—293.
44. Chatterjee S, Ganini D, Tokar EJ, et al. Leptin is key to peroxynitrite-mediated oxidative stress and Kupffer cell activation in experimental non-alcoholic steatohepatitis. *J Hepatol*. 2013;58(4):778—784.
45. Seki E, Schwabe RF. Hepatic inflammation and fibrosis: functional links and key pathways. *Hepatology*. 2015;61(3):1066—1079.
46. Novo E, Cannito S, Patemostro C, Bocca C, Miglietta A, Parola M. Cellular and molecular mechanisms in liver fibrogenesis. *Arch Biochem Biophys*. 2014;548:20—37.
47. Kucera O, Garnol T, Lotkova H, et al. The effect of rat strain, diet composition and feeding period on the development of a nutritional model of non-alcoholic fatty liver disease in rats. *Physiol Res*. 2011;60(2):317—328.